

SINGLE STEP FACILE SYNTHESIS OF SUPERPARAMAGNETIC IRON OXIDE NANOPARTICLES FOR CATALYTIC PYROLYSIS APPLICATIONS

M. RAZA^a, M. I. DIN^{a*}, S.ATA^a, H. A. MEHMOOD^b

Institute of Chemistry, University of the Punjab, Lahore, Pakistan, 54590

Department of Chemistry, GOVT.S.E College, Bahawalpur-63100, Pakistan

In this research work, Superparamagnetic iron oxide nanoparticles (SPION) were synthesized by a novel method from reduction of $\text{Fe}(\text{NO}_3)_3 \cdot 9\text{H}_2\text{O}$ precursor in three neck round bottom flask. For large scale synthesis, 8:1 (v/v) of $\text{Fe}(\text{NO}_3)_3 \cdot 9\text{H}_2\text{O}$ and cetyltrimethyl ammonium bromide solutions were mixed together, 5 mL of NaBH_4 solution added to mixture and then maintained the pH of the mixture at 12 by adding solution of NaOH drop wise. The morphology of prepared nanoparticles was determined by using scanning electron microscope (SEM). Size and crystallinity of nanoparticles was (10-12nm) investigated by diffractogram obtained from XRD. These particles were used as catalyst in the pyrolysis of nut-shell waste to produce alternative fuel and other chemicals feedstock for industrial applications. FT-IR analysis of nut-shell waste revealed the existence of lignocellulosic compounds. The effect of temperature on conversion of biomass into products and on percentage yield of products was also studied.

(Received September 16, 2017; Accepted December 7, 2017)

Keywords: Iron oxide nanoparticles; Alternative fuel; Catalytic pyrolysis

1. Introduction

There are different physical and chemical methods for the fabrication of nanoparticles. The two frequently used approaches are followed for the synthesis of nanoparticles. Amongst them, the high cost, top down method is used for the scale up synthesis, but it is a slow physical method [1]. The second one is a chemical approach termed as bottom up approach which is a fast and cost-effective method employed for the synthesis of nanoparticles. However, scale up synthesis cannot be performed by utilizing this technique [2].

Various other chemical and physical methods are employed for the synthesis of nanoparticles such as solvent evaporation method [3], arc discharge method [4], pulse laser ablation[5], hydrothermal process[6], co-precipitation method and sol gel process[7] etc. In solvent evaporation method [5], the precursor is vaporized by external heating source followed by rapid condensation. Physical vapor condensation method is applied in case of same composition of target material and nanoparticles. The chemical methods are preferred over physical methods if the composition of nanoparticles and target materials is dissimilar. High purity product is achieved by this method but at the compromised rate of reaction [8]. In arc discharge method, the target metal is injected in graphite electrode by piercing and then tremendously high temperature environment is provided. Metal carbides and magnetic metal-filled carbon Nanotubes are frequently synthesized by using this method. Cathode is made up of carbon nanotubes, fullerence, nanowires and nanoparticles while the anode is composed of certain metal catalyst. High quality particles are obtained by this method but the requirement of high temperature imposes a drawback of energy consumption [9].

Pulse laser ablation is a constructive approach to synthesize nanoparticles from organometallic precursors. An interface of laser photons and the gaseous reactant or sensitizer happens to take place in the laser pyrolysis, where the sensitizer is an energy transferring material. Very fine nanoparticles can be fabricated by this method where the size ranges from 2nm to 40nm

*Corresponding author: imrandin2007@gmail.com

but the underlying mechanism for the production of nanoparticles is not entirely explored yet. Uniform sized particles can be obtained by using this method while, the particles size can also be controlled on the other hand. By the Power of laser as well as mole ratio of oxygen or carrier gas [10] can control the crystallinity and size of particles.

Aqueous solutions or vapors can be made to react with the solid material at high pressure and temperature using solvothermal or hydrothermal methods. All inorganic precursors solubilize in water at elevated temperature and hence crystallization occurs. Initially amorphous polymeric hydroxides of metals cations are obtained during hydrothermal process. Further heating of these hydroxides leads to their dehydration and consequently metal oxide crystals are formed. The equipment which is used in this method is costly and crystal growth cannot be monitored [11] during the whole process.

Sol-gel method is a convenient technique used to synthesize nanoparticles consisting of particles insulating with the required optical and magnetic properties. The sol-gel method is depending on thermal decomposition, polycondensation, hydrolysis, drying and inorganic polymerization while water or alcohol is used to hydrolyze precursor. Since the properties of final product depend upon the rate of condensation and hydrolysis, the controlled and slower hydrolysis generate smaller sized particles featuring unique characteristics. Calcination at high temperature is usually followed after the condensation of solution to a gel. Hence the solvent might be eliminated along with the decomposition of organic precursor. High reaction rates are observed for the synthesis of particles by using sol-gel method. However, the use of expensive raw materials and loss of large amount of materials during drying [12] makes it a costly method. Co-precipitation method utilizes the solutions of salts of precursors whereas the pH is maintained by alkaline solutions. The subsequent heating under controlled conditions is performed followed by addition of reducing and capping agents. Firstly, this method was reported by Massart. This technique has numerous advantages; least cost of precursors, ease of handling and large number of products obtained in short time interval. But the process yields broader sized particles and their shape cannot be controlled through this method [13].

Magnetic properties associated with iron oxide NP's makes them to offer extensive applications in different fields including Ferrofluids, magnetic recording media, catalyst, magnetic inks and seals. They are also used as therapeutic agents in cancer treatment as well as a contrast agent in magnetic resonance imaging (MRI). These applications are based on magnetic properties, surface area, shape and size of NP's. Higher coercivity values feature magnetic nanoparticles to be used in data storage devices for instance video tapes, audio tapes [14] and magnetic discs. Magneto resistance behavior is executed upon mixing of nonmagnetic matrix with magnetite nanoparticles. Due to this behavior, it is used in magnetometers and magnetic recording heads.

Ferrofluids are suspensions of magnetic nanoparticles in aqueous medium or in organic solvents. Ferrofluids find applications in optical switches, tunable diffraction gratings and high efficient seals in space applications, NMR probes and are used to repair damaged retina in the surgery of eyes. Magnetite nanoparticles have superparamagnetic behavior; hence these are used in MRI, drug delivery and in development of immunoassays. Their low toxicity and high biocompatibility features them to offer extensive biological applications such as these are used for the detection of protein binding target to the double helical structure of DNA [15].

NP's of iron are also used to control the environmental pollution. In the treatment of polluted water, these are used to eliminate the chemical and industrial effluents, heavy metals and other toxic substances. Iron oxide nanoparticles are efficient catalysts of industrial importance for the manufacture of ammonia that in turn is also used as a catalyst. These are used further as catalyst in dehydrogenation reaction, oxidation of alcohols, synthesis of hydrocarbons, and many other oxidation and reduction reactions [16]. These are very effective catalyst for the pyrolysis of biomass to produce bio fuels. Their particle size and surface area makes them efficient catalyst to break down the cellulose and hemicellulose into the lower hydrocarbons and olefins. Lignocellulosic compounds are found in the waste obtained from nutshell. These lignocellulosic compounds thermally decompose into biofuels and chemical feedstock in the presence of catalyst. Iron NP's can be used for catalytic pyrolysis of nutshell. The continuous consumption of fossil fuels is depleting the natural reserves of fossil fuels with the passage of time. Therefore, it is necessary to explore the alternate, renewable, and clean source of energy. Biomass is also an

alternate and ecofriendly source of energy that emits low levels of carbon dioxide and negligible Sulphur amounts.

2. Experimental

2.1. Materials

All chemicals used are analytical graded and no more purification is required. Iron nitrate nonahydrate ($\text{Fe}(\text{NO}_3)_3 \cdot 9\text{H}_2\text{O}$ 0.1 M), sodium hydroxide (NaOH) 3M, sodium borohydride (NaBH_4) 10 wt % as reducing agent and cetyltrimethyl ammonium bromide (CTAB) 2.5 wt % all these chemicals were provided by Sigma-Aldrich.

2.2. Experimental procedures

4.04 g $\text{Fe}(\text{NO}_3)_3 \cdot 9\text{H}_2\text{O}$ was dissolved in 100 mL of deionized water to prepare 0.1 M solution. 3 M solution of sodium hydroxide was prepared by dissolving 3g NaOH in 100 mL deionized water. 10 % wt and 2.5 % wt solutions of sodium borohydride and CTAB were prepared. In this method 8:1 (v/v) of $\text{Fe}(\text{NO}_3)_3 \cdot 9\text{H}_2\text{O}$ and CTAB solutions were mixed together, 5 mL of NaBH_4 solution added to mixture and then maintained the pH of the mixture at 12 by adding solution of NaOH drop wise. The solution became turbid with dark brown precipitations on adding NaOH solution. Then the solution was refluxed for 3 hours at 100 °C on hot plate with continuous stirring. The prepared precipitates were separated and purified by centrifugation with the speed of 3000 rpm for 20 minutes and washed with ethanol and water. After washing, the separated and purified precipitate (ppt) were kept in the oven to proper dry for 6 hours at the temperature of 90 °C. Calcination of dried precipitates was performed at 600 °C for 1 hour in muffle furnace. The calcined precipitates were used for characterizations and as catalyst for the pyrolysis of nut-shells.

2.3. Nut-shells as biomass material

Nut-shell waste was used as biomass in pyrolysis to produce bio-oil and other products. Dry nut-shells were grinded into powder form. For the identification of structural groups present in biomass Cary 630 FT-IR model was used. FT-IR spectra of raw material are given in fig.1. The spectral bands of nut-shell raw material give the identification of cellulose, hemicellulose and lignin [17, 18]. The absorption peak at 1735 cm^{-1} give the identification of xylans of hemicellulose. The peaks of absorption at 2940 cm^{-1} , 1248 cm^{-1} represent the cellulose. The peaks at $650\text{--}850\text{ cm}^{-1}$, $1300\text{--}1400\text{ cm}^{-1}$, $1500\text{--}1600\text{ cm}^{-1}$, and 2900 cm^{-1} are the characteristics of lignin. The absorption characteristic peaks assure the presence of lignin, hemicellulose and cellulose in the nut shell raw material.

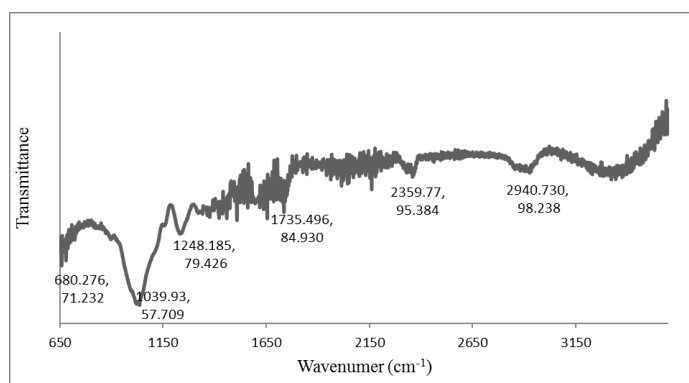


Fig. 1. FT-IR spectra of raw material (nut-shells)

2.4. Pyrolysis procedures

The pyrolysis experiments were carried out in a fixed-bed reactor made up of stainless steel. The schematic diagram of fixed-bed reactor is given in fig.2. In each experiment 20 g of biomass was taken in the reactor and tightly closed the reactor with the supply of inert gas and product output pipes are immersed in sample collecting bottles placed in ice to keep the

temperature low for condensation of gasses. The heat is provided to the reactor by external electric furnace. The experiments of pyrolysis were performed in three series. In first experiment, the pyrolysis was performed without catalyst at three different temperatures 350,400 and 450°C. The second pyrolysis experiment was performed by taking 5 mg catalyst (Fe_3O_4) inside the bed reactor at the same above mentioned temperature [18]. In third series 10 mg of Fe_3O_4 was taken in reactor as catalyst. The liquids condensed products were collected in bottles contain pyrolytic oil phase and aqueous pyrolignic acid. The oil phase was separated from pyrolignic acid in separating funnel by mixing dichloromethane. Anhydrous sodium sulphate was used to remove the moisture from separated bio-oil and recovered by solvent evaporation in rotatory evaporator at 40 °C 11 KPa pressure. The percentage yields of bio-oil, solid biochar was calculated by applying following equations:

$$\text{Conversion (\%)} = \frac{W(\text{biomss})-W(\text{biochar})}{W(\text{bimass})} \times 100 \quad (1)$$

$$\text{Liquid yield (wt\%)} = \frac{W(\text{liquid})}{W(\text{dry biomass})} \times 100 \quad (2)$$

$$\text{Solid yield (wt\%)} = \frac{W(\text{char})}{W(\text{dry biomass})} \times 100 \quad (3)$$

$$\text{Gas yield (wt\%)} = 100 - (\text{liquid bio-oil yield} + \text{char yield}) \quad (4)$$

3. Results and discussions

3.1. X-ray diffraction

Chemically synthesized Fe_3O_4 nanoparticles diffractogram is shown in fig.3. The peaks of diffraction indicate the presence of inverse cubic spinal phase of magnetite Fe_3O_4 [19]. In addition, the sharp and intense peaks show the crystallinity of nanoparticles. The purity of Fe_3O_4 NP's is also indicated from X-RAY diffractogram, there is no peak corresponding to impure phase. The average crystallite size of Fe_3O_4 NP's was determined by using Debye-Scherrer's equation [20].

$$D = \frac{K\lambda}{\beta \cos\theta}$$

Where D = size of grain (nm), K = constant (0.98), λ = wavelength of X-rays (1.54 Å), β = full width at half maximum (FWHM) and θ = angle of diffraction.

By using Scherrer's equation, the average size of Fe_3O_4 was calculated from this peak was ~ 10 nm.

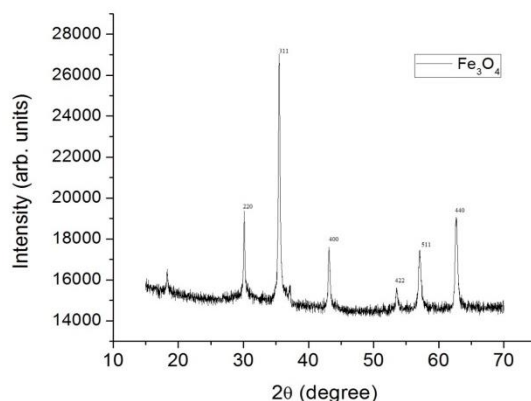


Fig.3 X-ray diffractogram of Fe_3O_4 nanoparticles

The sharp and strong reflection peaks reveal the crystallinity of the magnetite nanoparticles. The baseline is smooth and narrower half-peak breadth represents the absence of any noncrystalline materials in the nanoparticles.

3.2. SEM-images of Fe_3O_4 nanoparticles

SEM image of prepared Fe_3O_4 nanoparticles is given in fig.4. Scanning electron microscope (SEM) was used to evaluate the morphology of the particles. The image was obtained at 30 kV of accelerating voltage using 6.1 mm working distance and 3.0 nm spot size [21].

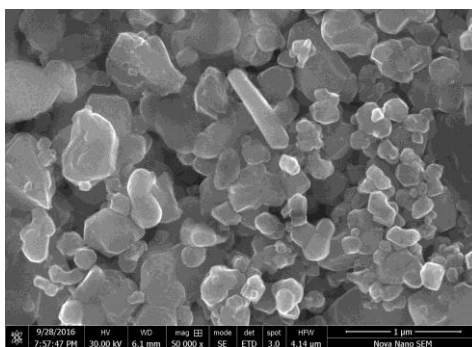


Fig.4 SEM image of Fe_3O_4 nanoparticles

3.3. Percentage yields of pyrolytic products

Three main products are produced from the pyrolysis of biomass namely liquid bio-oil, non-condensed gases and solid bio-char. The effect of temperature and catalyst on conversion and products yield was studied and shown in figure 5a and 5b. The bio-oil yield is maximized by increasing temperature and catalyst but the yield of gases is also increased by increasing temperature. The amount of solid bio-char decreases by increasing temperature and catalyst. The percentage yields of conversion, liquid bio-oil, gas and solid char at different temperature and catalyst are given in tables 1-3.

Table 1: percentage of conversion, liquid bio-oil, gas yield and char without catalyst

Temperature	Conversion %	Liquid bio-oil %	Gas yield %	Solid bio-char %
350 °C	65	30	25	45
400 °C	73	32	31	37
450 °C	74	31	33	36

Table 2: percentage of conversion, liquid bio-oil, gas yield and char with 5 mg Fe_3O_4

Temperature	Conversion %	Liquid bio-oil %	Gas yield %	Solid bio-char %
350 °C	67	31	22	47
400 °C	74	32	29	39
450 °C	75	31.5	30.5	38

Table 3: percentage of conversion, liquid bio-oil, gas yield and char with 10 mg Fe_3O_4

Temperature	Conversion %	Liquid bio-oil %	Gas yield %	Solid bio-char %
350 °C	69	32	19	49
400 °C	76	34	25	41
450 °C	77	32	28	40

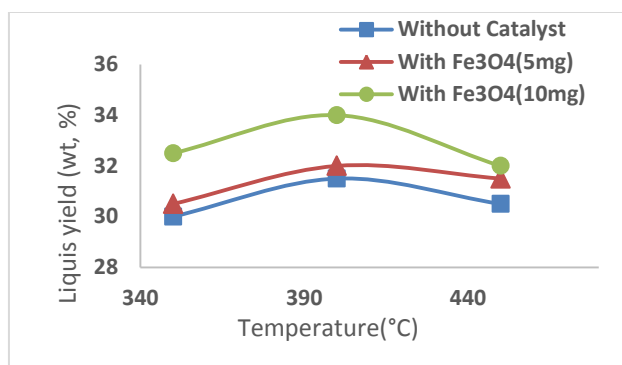


Fig 5a: The effect of temperature and catalyst on conversion percentage

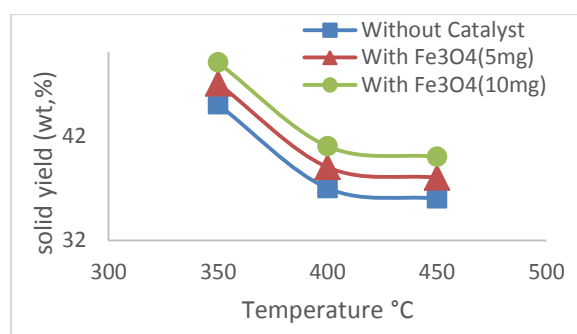


Fig 5: The effect of catalyst and temperature on solid yield (wt, %)

4. Conclusion

Fe₃O₄ nanoparticles are synthesized chemically using solution of iron nitrate nonahydrate (Fe₃O₄.9H₂O) as precursor, CTAB as capping agent and NaBH₄ as reducing agent. The size of prepared nanoparticles was approximately 10 nm, determined from diffractogram by using scherrer's equation. The morphology of synthesized nanoparticles was determined by image taken from scanning electron microscope. Nut-shell waste was used to produce bio-oil by pyrolysis at 350, 400, 450 °C temperatures. Prepared magnetite nanoparticles were used as catalyst for the pyrolysis of nut-shells. The effect of temperature and catalyst on pyrolytic conversions and products yield was investigated comparatively.

References

- [1] A.K. Gupta, M. Gupta, Biomaterials, **26**, 3995 (2005).
- [2] T. Hyeon, Chemical synthesis of magnetic nanoparticles, Chemical Communications, 927 (2003).
- [3] C. P. Reis, R. J. Neufeld, A. J. Ribeiro, F. Veiga, Biology and Medicine **2**, 8 (2006).
- [4] A. Ashkarran, M. Ahadian, S.M. Ardakani, Nanotechnology, **19**, 195709 (2008).
- [5] D. B. Geohegan, A. A. Puretzky, G. Duscher, S.J. Pennycook, Applied Physics Letters **72**, 2987(1998).
- [6] Q. Lu, F. Gao, D. Zhao, Nano letters **2**, 725 (2002).
- [7] B.G. Trewyn, I.I. Slowing, S. Giri, H.-T. Chen, V.S.-Y. Lin, Accounts of chemical research, **40**, 846(2007).
- [8] M. Zambaux, F. Bonneaux, R. Gref, P. Maincent, E. Dellacherie, M. Alonso, P. Labrude, C. Vigneron, I Journal of Controlled Release, **50**, 31 (1998).
- [9] J. Jiao, S. Seraphin, X. Wang, J.C. Withers, Journal of Applied Physics, **80**,103 (1996).

- [10] M.C. Bautista, O. Bomati-Miguel, M. del Puerto Morales, C.J. Serna, S. Veintemillas-Verdaguer, *Journal of Magnetism and Magnetic Materials* **293**, 20 (2005).
- [11] W. Wu, Q. He, C. Jiang, *Nanoscale research letters* **3**, 397 (2008).
- [12] J. Xu, H. Yang, W. Fu, K. Du, Y. Sui, J. Chen, Y. Zeng, M. Li, G. Zou, *Journal of Magnetism and Magnetic Materials* **309**, 307 (2007).
- [13] N. Kandpal, N. Sah, R. Loshali, R. Joshi, J. Prasad, Co-precipitation method of synthesis and characterization of iron oxide nanoparticles, (2014).
- [14] A.S. Teja, P.-Y. Koh, *Progress in crystal growth and characterization of materials*, **55**, 22 (2009).
- [15] J. Park, E. Lee, N. M. Hwang, M. Kang, S.C. Kim, Y. Hwang, J.G. Park, H.J. Noh, J.Y. Kim, J.H. Park, *Angewandte Chemie* **117**, 2932 (2005).
- [16] N. Lee, T. Hyeon, *Chemical Society Reviews* **41**, 2575 (2012).
- [17] A. Kumar, H.M. Jena, *Applied Surface Science* **356**, 753 (2015).
- [18] A. Aho, N. Kumar, K. Eränen, T. Salmi, M. Hupa, D.Y. Murzin, *Fuel* **87**, 2493 (2008).
- [19] R. Hong, B. Feng, L. Chen, G. Liu, H. Li, Y. Zheng, D. Wei, *Biochemical Engineering Journal* **42**,290(2008).
- [20] X. Jiang, A. Yu, *Journal of Materials Processing Technology* **209**, 4558 (2009).
- [21] J. Chen, L. Xu, W. Li, X. Gou, *Advanced Materials* **17**, 582 (2005).